

# $\Sigma_c \Sigma_c$ interactions in chiral effective field theory

Kan Chen,<sup>1</sup> Bo-Lin Huang,<sup>1</sup> Bo Wang,<sup>2,\*</sup> and Shi-Lin Zhu<sup>1,†</sup>

<sup>1</sup>*School of Physics and Center of High Energy Physics, Peking University, Beijing 100871, China*

<sup>2</sup>*School of Physical Science and Technology, Hebei University, Baoding 071002, China*

*Key Laboratory of High-precision Computation and Application of Quantum Field Theory of Hebei Province, Baoding 071002, China*

We study the interactions of the  $\Sigma_c \Sigma_c$  system in the framework of chiral effective theory. We consider the contact, one-pion and two-pion exchange interactions and bridge the low energy constants of the  $\Sigma_c \Sigma_c$  system to those of the  $\Sigma_c^{(*)} \bar{D}^{(*)}$  systems through the quark-level ansatz for the contact interaction. We explore the influence of intermediate channels in the two-pion exchange diagrams of the  $\Sigma_c \Sigma_c$  system. We obtain a deep bound state  $[\Sigma_c \Sigma_c]_{J=0}^{I=0}$  and a shallow bound state  $[\Sigma_c \Sigma_c]_{J=1}^{I=1}$ . As a byproduct, we further investigate the interactions of the  $\Lambda_c \Lambda_c$  and  $\Lambda_c \Sigma_c$  systems.

## I. INTRODUCTION

The quark model described the conventional mesons and baryons quite well [1, 2]. However, since the discoveries of the  $D_{s0}^*(2317)$  [3] and  $X(3872)$  [4] in 2003, a large number of states that cannot be classified into conventional hadrons are continuously reported [5]. Different pictures have been proposed to understand the nature of these exotic states, such as the compact multiquark states, loosely bound hadronic molecules, and kinetic effects, etc [6–15]. Many exotic states are near the thresholds of a pair of heavy hadrons from several to several tens MeVs, which makes the hadronic molecular picture the popular one.

The hidden-charm pentaquarks were first reported in the  $\Lambda_b^0 \rightarrow J/\psi p K^-$  process by the LHCb Collaboration [16, 17]. In 2019, the updated analysis with about 10 times larger statistics showed that there exist three pronounced states  $P_c(4312)$ ,  $P_c(4440)$ , and  $P_c(4457)$  in the  $J/\psi p$  invariant mass spectrum [18]. Since the masses of the reported pentaquarks are below the thresholds of the  $\Sigma_c \bar{D}^{(*)}$  systems, the molecular explanations of these states have been discussed in lots of works [19–32]. After the observation of  $P_c$  states, their strange partners were studied in Refs. [33–38]. The  $P_{cs}$  states were experimentally investigated in the  $\Xi_b^- \rightarrow J/\psi \Lambda K^-$  process by the LHCb [39]. They reported the evidence of a new pentaquark state  $P_{cs}(4459)$  with  $3\sigma$  significance. Besides, the LHCb Collaboration [40] also showed the evidence of a  $P_c(4337)^+$  signal from their four-dimensional amplitude analysis in the  $B_s^0 \rightarrow J/\psi p \bar{p}$  process with less than  $4\sigma$  significance. Very recently, the LHCb Collaboration reported a very narrow structure  $T_{cc}^+(3875)$  in the  $D^0 D^0 \pi^+$  invariant spectrum [41, 42]. This state lies slightly below the  $D^{*+} D^0$  threshold by about 300 keV. Before the observation of  $T_{cc}^+(3875)$ , the  $QQ\bar{q}\bar{q}$  configurations had been studied by many works based on the tetraquark picture [43–56] or the molecular scenario [57–69].

It is natural to investigate the existence of molecular states that are composed of two baryons. Up to now, the deuteron is the only well-established molecule composed of a proton

and a neutron. Although the  $\Lambda\Lambda$  di-baryon state was predicted long ago by Jaffe [70] and received amounts of attentions [71–78], the existence of this state is still controversial. The di-baryon systems that are composed of two charmed baryons are more likely to be bound, since the large reduced mass can facilitate the stabilization of such systems. As the heavy flavor siblings of the nucleon, the molecular states in the  $\Sigma_c \Sigma_c$  system have been investigated in a series of works [79–85]. In this work, we will mainly concentrate on the interactions of the  $\Sigma_c \Sigma_c$  system, and explore the relevance of intermediate states in the two-pion exchange (TPE) loops within the chiral effective field theory ( $\chi$ EFT). In addition, we will also study the interactions of the  $\Lambda_c \Lambda_c$  and  $\Lambda_c \Sigma_c$  systems. The  $\Lambda_c \Lambda_c$  system was studied in various models [79–81, 83, 86–92]. It was shown that the single-channel  $\Lambda_c \Lambda_c$  cannot form the bound state [79–81, 83, 84, 90, 91], while in Refs. [86, 88, 89, 92] the authors argued that the coupling to the attractive  $\Sigma_c^{(*)} \Sigma_c^{(*)}$  channels may lead the  $\Lambda_c \Lambda_c$  system to be bound. The  $\Lambda_c \Sigma_c$  molecules were studied in the one-boson-exchange model [86] and the dispersion relation technique [81], while the  $\Lambda_c \Sigma_c$  bound states were disfavored in Ref. [83]. The calculations and discussions on the  $\Lambda_c \Sigma_c$  and  $\Lambda_c \Lambda_c$  interactions are relegated to the appendix A in this work.

The chiral effective field theory ( $\chi$ EFT) has been widely applied to describe the nuclear forces (see [93–97] for reviews), as well as the  $D_s(2317)$  [98],  $T_{cc}$  [99],  $P_c$  [26, 32], and  $P_{cs}$  [37] states (see the recent review [15]). In the framework of  $\chi$ EFT, we include the leading order (LO) contact term, one-pion exchange (OPE), and two-pion exchange (TPE) contributions to account for the short-, long-, and intermediate-range interactions of the doubly charmed di-baryon systems, respectively. Among them, the OPE and TPE interactions (loops are calculated with the dimensional regularization scheme) can be derived from the chiral Lagrangians, and their contributions are definite since the involved coupling constants can be determined from experiments. The meson-meson ( $\bar{c}q$ )-( $\bar{c}q$ ), baryon-meson ( $cqq$ )-( $\bar{c}q$ ), and baryon-baryon ( $cqq$ )-( $cqq$ ) systems are composed of (anti)charm quarks and light quarks (without light antiquarks), thus the exchanged light currents may play very similar dynamic roles in the heavy quark limit [100, 101]. Therefore, for the undetermined short-range contact interactions, they can be related to each other via a quark level Lagrangian [37, 100–103] since they are re-

\* wangbo@hbu.edu.cn

† zhushl@pku.edu.cn

quired to obey the SU(3) flavor symmetry and heavy quark symmetry.

This paper is organized as follows. In Sec. II, we present the chiral effective Lagrangians and the effective potentials. In Sec. III, we present our numerical results and discussions. In Sec. IV, we conclude this work with a short summary. We present the results for the  $\Lambda_c \Lambda_c$  and  $\Lambda_c \Sigma_c$  systems in appendix A.

## II. CHIRAL EFFECTIVE LAGRANGIANS AND EFFECTIVE POTENTIALS

### A. Chiral effective Lagrangians

In the SU(2) case, the light diquark in the ground-state singly charmed baryons can be the antisymmetric isosinglet or symmetric isotriplet. The corresponding total spin of the light diquark component is  $j_l = 0$  or  $j_l = 1$ . The spin- $\frac{1}{2}$  isosinglet is defined as

$$\psi_1 = \begin{bmatrix} 0 & \Lambda_c^+ \\ -\Lambda_c^+ & 0 \end{bmatrix}, \quad (1)$$

$$\begin{aligned} \mathcal{L}_{\mathcal{B}\varphi} = & \frac{1}{2} \text{Tr} [\mathcal{B}_1 (i v \cdot D) \mathcal{B}_1] + 2g_2 \text{Tr} (\bar{\mathcal{B}}_3 \mathcal{S} \cdot u \mathcal{B}_1 + \text{H.c.}) + g_3 \text{Tr} (\bar{\mathcal{B}}_{3^*}^\mu u_\mu \mathcal{B}_3 + \text{H.c.}) + g_4 \text{Tr} (\bar{\mathcal{B}}_{3^*}^\mu u_\mu \mathcal{B}_1 + \text{H.c.}) \\ & + \text{Tr} [\bar{\mathcal{B}}_3 (i v \cdot D - \delta_c) \mathcal{B}_3] + 2g_5 \text{Tr} (\bar{\mathcal{B}}_{3^*}^\mu \mathcal{S} \cdot u \mathcal{B}_{3^*}^\mu) - \text{Tr} [\bar{\mathcal{B}}_{3^*}^\mu (i v \cdot D - \delta_d) \mathcal{B}_{3^* \mu}] + 2g_1 \text{Tr} (\bar{\mathcal{B}}_3 \mathcal{S} \cdot u \mathcal{B}_3), \end{aligned} \quad (4)$$

where  $\mathcal{S}^\mu = \frac{i}{2} \gamma_5 \sigma^{\mu\nu} v_\nu$  is the covariant spin operator for the spin- $\frac{1}{2}$  baryon. The covariant derivative  $D_\mu \psi = \partial_\mu \psi + \Gamma_\mu \psi + \psi \Gamma_\mu^T$ , with  $\Gamma_\mu^T$  the transpose of  $\Gamma_\mu$ . The chiral connection  $\Gamma_\mu$  and axial-vector current  $u_\mu$  are defined as

$$\Gamma_\mu = \frac{1}{2} [\xi^\dagger, \partial_\mu \xi], \quad u_\mu = \frac{i}{2} \{\xi^\dagger, \partial_\mu \xi\}, \quad (5)$$

with

$$\xi^2 = U = \exp \left( \frac{i\varphi}{f_\pi} \right), \quad \varphi = \begin{bmatrix} \pi^0 & \sqrt{2}\pi^+ \\ \sqrt{2}\pi^- & -\pi^0 \end{bmatrix}, \quad (6)$$

$$\begin{aligned} \mathcal{L}_{\mathcal{B}\mathcal{B}} = & C_a \text{Tr} (\bar{\mathcal{B}}_1 \mathcal{B}_1) \text{Tr} (\bar{\mathcal{B}}_1 \mathcal{B}_1) + C_b \text{Tr} (\bar{\mathcal{B}}_1 \mathcal{B}_1) \text{Tr} (\bar{\psi}^\mu \psi_\mu) + C_c \text{Tr} (\bar{\psi}^\mu \psi_\mu) \text{Tr} (\bar{\psi}^\nu \psi_\nu) + D_a \text{Tr} (\bar{\psi}^\mu \tau_i \psi_\mu) \text{Tr} (\bar{\psi}^\nu \tau^i \psi_\nu) \\ & + i C_d \epsilon_{\mu\nu\alpha\beta} v^\alpha \text{Tr} (\bar{\psi}^\rho \gamma^\beta \gamma_5 \psi_\rho) \text{Tr} (\bar{\psi}^\mu \psi^\nu) + i D_b \epsilon_{\mu\nu\alpha\beta} v^\alpha \text{Tr} (\bar{\psi}^\rho \gamma^\beta \gamma_5 \tau^i \psi_\rho) \text{Tr} (\bar{\psi}^\mu \tau_i \psi^\nu), \end{aligned} \quad (7)$$

where we use the super-field notation for the heavy quark spin doublet  $(\mathcal{B}_3, \mathcal{B}_{3^*})$ ,

$$\psi^\mu = \mathcal{B}_{3^*}^\mu - \frac{1}{\sqrt{3}} (\gamma^\mu + v^\mu) \gamma^5 \mathcal{B}_3, \quad \text{and} \quad \bar{\psi}^\mu = \bar{\mathcal{B}}_{3^*}^\mu + \frac{1}{3} \bar{\mathcal{B}}_3 \gamma^5 (\gamma^\mu + v^\mu). \quad (8)$$

The  $C_a, C_b, C_c, D_a, C_d$ , and  $D_b$  are six independent low-energy constants (LECs) that will be determined later.  $\tau^i$  represents the isospin Pauli matrix. Note that the other forms of the LO contact Lagrangians with different Lorentz structures are also allowed, but they can be expressed as the linear combinations of the terms involved in Eq. (7).

### B. Effective potentials

Due to the symmetry constraint for the identical particles [100], the two  $\Sigma_c$  baryons can form

$$[\Sigma_c \Sigma_c]_J^I, \quad \text{with} \quad (J, I) = (0, 0), (1, 1), (0, 2). \quad (9)$$

while the spin- $\frac{1}{2}$  and spin- $\frac{3}{2}$  isospin triplets are defined as

$$\psi_3 = \begin{bmatrix} \Sigma_c^{++} & \frac{\Sigma_c^+}{\sqrt{2}} \\ \frac{\Sigma_c^+}{\sqrt{2}} & \Sigma_c^0 \end{bmatrix}, \quad \psi_{3^*}^\mu = \begin{bmatrix} \Sigma_c^{*++} & \frac{\Sigma_c^{*+}}{\sqrt{2}} \\ \frac{\Sigma_c^{*+}}{\sqrt{2}} & \Sigma_c^{*0} \end{bmatrix}^\mu. \quad (2)$$

In the heavy baryon reduction formalism [104], the heavy baryon field can be decomposed into the light and heavy components through the projection operators  $(1 \pm \not{v})/2$ ,

$$\mathcal{B}_i = e^{iM_i v \cdot x} \frac{1 + \not{v}}{2} \psi_i, \quad \mathcal{H}_i = e^{iM_i v \cdot x} \frac{1 - \not{v}}{2} \psi_i, \quad (3)$$

with  $\psi_i$  the heavy baryon fields  $\psi_1, \psi_3, \psi_{3^*}^\mu$ , and  $M_i$  the masses of heavy baryons. The four-velocity  $v_\mu = (1, \mathbf{0})$  in the rest frame of the heavy baryons. In the leading order expansion, only the light component  $\mathcal{B}_i$  is kept.

Then we introduce the leading order chiral Lagrangians to describe the interactions between the charmed baryons and pion fields [105, 106]

in which  $f_\pi = 92.4$  MeV is the pion decay constant.

The coupling constants  $g_2 = -0.6$  and  $g_4 = 1.04$  in Eq. (4) are determined from the partial decay widths of the  $\Sigma_c \rightarrow \Lambda_c \pi$  and  $\Sigma_c^* \rightarrow \Lambda_c \pi$  [5], respectively. The other coupling constants  $g_1 = 0.98, g_3 = 0.85$ , and  $g_5 = -1.47$  are obtained by relating them to  $g_2$  via the quark model [89, 107, 108]. The mass splittings  $\delta_a = M_{\Sigma_c^*} - M_{\Sigma_c} = 65$  MeV,  $\delta_b = M_{\Sigma_c} - M_{\Lambda_c} = 168.5$  MeV, and  $\delta_c = M_{\Sigma_c^*} - M_{\Lambda_c} = 233.5$  MeV are extracted from the masses of the  $\Lambda_c, \Sigma_c$ , and  $\Sigma_c^*$  baryons [5].

The following Lagrangian is constructed to describe the four-body contact interactions (FBCI) among  $\mathcal{B}_1, \mathcal{B}_3$  and  $\mathcal{B}_{3^*}$ ,

In what follows the subscript and superscript denote the total spin and isospin of the corresponding di-baryon systems,

respectively.

The scattering amplitude  $\mathcal{M}(\mathbf{q})$  can be calculated by expanding the Lagrangians in Eqs. (4)-(7). It can be related to the effective potential under the Breit approximation, i.e.,

$$\mathcal{V}(\mathbf{q}) = -\frac{\mathcal{M}(\mathbf{q})}{\sqrt{2M_1 2M_2 2M_3 2M_4}}, \quad (10)$$

where the  $M_{1,2}$  and  $M_{3,4}$  are the masses of the incoming and outgoing particles, respectively.

The expressions for the LO contact and OPE potentials read

$$\begin{aligned} \mathcal{V}_{\Sigma_c \Sigma_c}^{\text{ct}} &= -4 [C_c + (\mathbf{I}_1 \cdot \mathbf{I}_2) D_a] \\ &+ \frac{8}{9} [C_d + (\mathbf{I}_1 \cdot \mathbf{I}_2) D_b] \boldsymbol{\sigma}_1 \cdot \boldsymbol{\sigma}_2, \end{aligned} \quad (11)$$

$$\mathcal{V}_{\Sigma_c \Sigma_c}^{\text{OPE}} = -(\mathbf{I}_1 \cdot \mathbf{I}_2) \frac{g_1^2 (\boldsymbol{\sigma}_1 \cdot \mathbf{q})(\boldsymbol{\sigma}_2 \cdot \mathbf{q})}{4f_\pi^2 (\mathbf{q}^2 + m_\pi^2)}, \quad (12)$$

in which the eigenvalues of the  $\mathbf{I}_1 \cdot \mathbf{I}_2$  and  $\boldsymbol{\sigma}_1 \cdot \boldsymbol{\sigma}_2$  operators can be calculated with the following equations

$$\langle \mathbf{I}_1 \cdot \mathbf{I}_2 \rangle = \frac{1}{2} [I(I+1) - I_1(I_1+1) - I_2(I_2+1)],$$

$$\langle \boldsymbol{\sigma}_1 \cdot \boldsymbol{\sigma}_2 \rangle = 2 [S(S+1) - S_1(S_1+1) - S_2(S_2+1)].$$

As shown in Eq. (11), the contact potential of the  $\Sigma_c \Sigma_c$  system consists of four parts—the central term, the isospin-isospin interaction term  $\mathbf{I}_1 \cdot \mathbf{I}_2$ , the spin-spin interaction term  $\boldsymbol{\sigma}_1 \cdot \boldsymbol{\sigma}_2$ , and the isospin-spin interaction coupled term  $(\mathbf{I}_1 \cdot \mathbf{I}_2)(\boldsymbol{\sigma}_1 \cdot \boldsymbol{\sigma}_2)$ . The contact and OPE potentials for the different  $\Sigma_c \Sigma_c$  states can be distinguished with the matrix elements of the isospin and spin operators. In the  $S$ -wave case, the operator  $(\boldsymbol{\sigma}_1 \cdot \mathbf{q})(\boldsymbol{\sigma}_2 \cdot \mathbf{q})$  can be simplified with the following replacement [64, 109]

$$(\boldsymbol{\sigma}_1 \cdot \mathbf{q})(\boldsymbol{\sigma}_2 \cdot \mathbf{q}) \rightarrow \frac{1}{3} \mathbf{q}^2 (\boldsymbol{\sigma}_1 \cdot \boldsymbol{\sigma}_2). \quad (13)$$

The NLO TPE diagrams for the  $\Sigma_c \Sigma_c$  system are illustrated in Fig. 1. The TPE diagrams include the football diagram ( $F_{1.1}$ ), triangle diagrams ( $T_{1.1}$ )-( $T_{1.6}$ ), box diagrams ( $B_{1.1}$ )-( $B_{1.9}$ ), and cross diagrams ( $R_{1.1}$ )-( $R_{1.9}$ ). The analytical expressions of the TPE potentials from these diagrams can be collectively written as

$$\mathcal{V}^{F_{1.1}} = (\mathbf{I}_1 \cdot \mathbf{I}_2) \frac{1}{f_\pi^4} J_{22}^F, \quad (14)$$

$$\mathcal{V}^{T_{1,j}} = (\mathbf{I}_1 \cdot \mathbf{I}_2) \frac{\mathcal{C}^{T_{1,j}}}{f_\pi^4} \left[ \mathbf{q}^2 C_1^{T_{1,j}} (J_{24}^T + J_{33}^T) + C_2^{T_{1,j}} J_{34}^T \right] (\mathcal{E}^{T_{1,j}}), \quad (15)$$

$$\begin{aligned} \mathcal{V}^{B_{i,j}} &= F_I^{B_{i,j}} \frac{\mathcal{C}^{B_{i,j}}}{f_\pi^4} \left[ \mathbf{q}^2 C_1^{B_{i,j}} J_{21}^B + \frac{2}{3} \mathbf{q}^2 C_2^{B_{i,j}} (\boldsymbol{\sigma}_1 \cdot \boldsymbol{\sigma}_2) J_{21}^B + \mathbf{q}^4 C_3^{B_{i,j}} (J_{22}^B + 2J_{32}^B + J_{43}^B) + C_5^{B_{i,j}} J_{41}^B \right. \\ &\quad \left. + \mathbf{q}^2 C_4^{B_{i,j}} (J_{31}^B + J_{42}^B) \right] (\mathcal{E}_1^{B_{i,j}}, \mathcal{E}_2^{B_{i,j}}), \end{aligned} \quad (16)$$

$$\begin{aligned} \mathcal{V}^{R_{i,j}} &= F_I^{R_{i,j}} \frac{\mathcal{C}^{R_{i,j}}}{f_\pi^4} \left[ \mathbf{q}^2 C_1^{R_{i,j}} J_{21}^R + \frac{2}{3} \mathbf{q}^2 C_2^{R_{i,j}} (\boldsymbol{\sigma}_1 \cdot \boldsymbol{\sigma}_2) J_{21}^R + \mathbf{q}^4 C_3^{R_{i,j}} (J_{22}^R + 2J_{32}^R + J_{43}^R) + C_5^{R_{i,j}} J_{41}^R \right. \\ &\quad \left. + \mathbf{q}^2 C_4^{R_{i,j}} (J_{31}^R + J_{42}^R) \right] (\mathcal{E}_1^{R_{i,j}}, \mathcal{E}_2^{R_{i,j}}), \end{aligned} \quad (17)$$

in which we have used Eq. (13) in Eqs. (16)-(17). The coefficients defined in Eq. (15) for the triangle diagrams are collected in Table I. The  $\Sigma_c \Sigma_c$  system can couple to isospin  $I = 0, 1, 2$ . The isospin factors  $F_I^{B_{i,j}}$  ( $F_I^{R_{i,j}}$ ) of the box (cross) diagrams defined in Eq. (16) [Eq. (17)] are collected in Table II. The other coefficients defined in Eq. (16) and Eq. (17) are given in Table III.

TABLE I. The coefficients defined in Eq. (15) for the  $\Sigma_c \Sigma_c$  system.

	$\mathcal{C}^{T_{1,j}}$	$C_1^{T_{1,j}}$	$C_2^{T_{1,j}}$	$\mathcal{E}^{T_{1,j}}$
$j = 1, 4$	$\frac{g_2^2}{2}$	1	3	$\delta_b$
$j = 2, 5$	$\frac{g_1^2}{4}$	1	3	0
$j = 3, 6$	$\frac{g_3^2}{6}$	1	3	$-\delta_a$

### III. NUMERICAL RESULTS AND DISCUSSIONS

#### A. Contact terms

The scalar loop functions  $J_{ab}^F$ ,  $J_{ab}^T$ ,  $J_{ab}^B$ , and  $J_{ab}^R$  defined in Eqs. (14)-(17) have been given in the Appendix of Refs. [26, 32]. The residual energies  $\mathcal{E}^{T_{i,j}}$ ,  $\mathcal{E}_{1(2)}^{B_{i,j}}$ ,  $\mathcal{E}_{1(2)}^{R_{i,j}}$  are defined as the mass differences of the incoming and intermediate states.

Since the experimental data or lattice QCD simulations for the interactions of the doubly charmed di-baryon systems are still absent, we have to use a practical way to estimate the LECs in Eq. (7). In Refs. [37, 100–103], we pro-

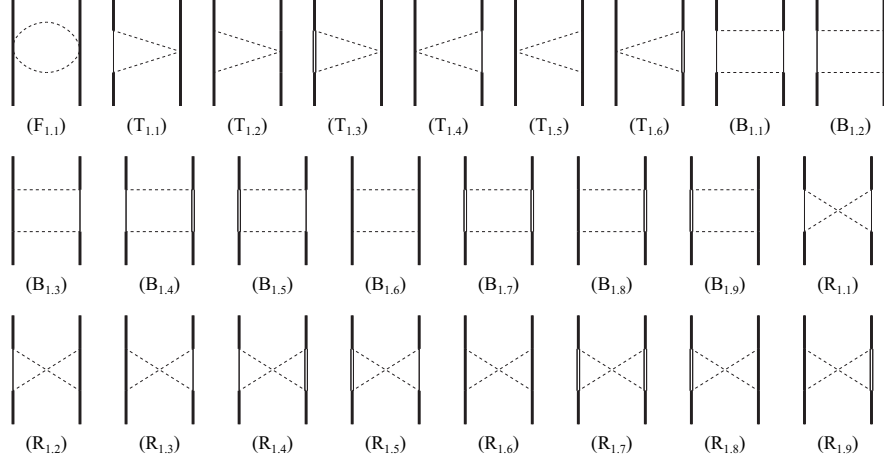


FIG. 1. TPE diagrams for the  $\Sigma_c \Sigma_c$  system at NLO. We use the thin line, thick line, double-thin line, and dashed line to denote the  $\Lambda_c$ ,  $\Sigma_c$ ,  $\Sigma_c^*$ , and  $\pi$ , respectively.

TABLE II. Isospin factors of the box and cross diagrams for the  $\Sigma_c \Sigma_c$  system defined in Eq. (16) and Eq. (17).

	$j = 1$	$j = 2, 3, 4, 5$	$j = 6, 7, 8, 9$
$[F_2^{\text{B}1.j}, F_1^{\text{B}1.j}, F_0^{\text{B}1.j}]$	[0, 0, 3]	[0, 2, 0]	[1, 1, 4]
$[F_2^{\text{R}1.j}, F_1^{\text{R}1.j}, F_0^{\text{R}1.j}]$	[1, -1, 1]	[1, 1, -2]	[2, 0, 2]

posed to bridge the unknown LECs to the systems with experimental data via a quark-level Lagrangian. This effective approach has been successfully used to predict the  $P_{cs}$  states [37]. In this approach, the contact interactions of the heavy flavor di-hadron systems are ascribed to the exchange of the light meson currents. The interactions induced by the light meson exchanges dominate the interactions of the heavy flavor di-hadron systems. The light quark components of the experimentally observed  $P_c$  states and the  $\Sigma_c \Sigma_c$  are all light quarks (without light antiquarks). Thus, the exchanged light mesons shall play very similar dynamic roles in the hidden-charm meson-baryon and double-charm di-baryon systems [100, 101]. Therefore, we can use the data of the  $P_c$  states as input to estimate the LECs of the  $\Sigma_c \Sigma_c$  system.

In Ref. [32], we presented a detailed study on the interactions of the  $\Sigma_c^{(*)} \bar{D}^{(*)}$  systems with  $\chi$ EFT. The LO contact terms of the  $[\Sigma_c \bar{D}^*]_{1/2}^{1/2}$  and  $[\Sigma_c \bar{D}^*]_{3/2}^{1/2}$  systems are given as [32]

$$\mathcal{V}_{[\Sigma_c \bar{D}^*]_{1/2}^{1/2}} = -\mathbb{D}_1 - \frac{4}{3}\mathbb{D}_2, \quad (18)$$

$$\mathcal{V}_{[\Sigma_c \bar{D}^*]_{3/2}^{1/2}} = -\mathbb{D}_1 + \frac{2}{3}\mathbb{D}_2, \quad (19)$$

where we adopt the same notations as that of Ref. [32]. The  $\mathbb{D}_1$  and  $\mathbb{D}_2$  are two LECs denoting the strength of the central potential and spin-spin interaction, respectively. Two sets of solutions for  $\mathbb{D}_1$  and  $\mathbb{D}_2$  were obtained in Ref. [32] via fitting

the binding energies of  $P_c$  states, here, we adopt

$$\Lambda = 0.5 \text{ GeV}, \quad \begin{cases} \mathbb{D}_1 = 52.0 \text{ GeV}^{-2}, \\ \mathbb{D}_2 = -4.0 \text{ GeV}^{-2}, \end{cases} \quad (20)$$

where  $\Lambda$  is the cutoff that will be introduced in Eq. (26). On the other hand, the expressions of the quark-level contact terms for the  $[\Sigma_c \bar{D}^*]_{1/2}^{1/2}$  and  $[\Sigma_c \bar{D}^*]_{3/2}^{1/2}$  can be written as

$$\mathcal{V}_{[\Sigma_c \bar{D}^*]_{1/2}^{1/2}} = -\frac{10}{3}\tilde{g}_s + \frac{40}{9}\tilde{g}_a, \quad (21)$$

$$\mathcal{V}_{[\Sigma_c \bar{D}^*]_{3/2}^{1/2}} = -\frac{10}{3}\tilde{g}_s - \frac{20}{9}\tilde{g}_a, \quad (22)$$

in which the notations for the quark-level couplings  $\tilde{g}_s$  and  $\tilde{g}_a$  are the same as those of Ref. [100]. One can easily obtain the values of  $\tilde{g}_s$  and  $\tilde{g}_a$  through matching Eqs. (21), (22) and Eqs. (18), (19). In Ref. [100], we only used the LO contact terms to model the effective potentials of the  $\Sigma_c^{(*)} \bar{D}^{(*)}$  systems. In this case, the estimated  $\tilde{g}_s$  and  $\tilde{g}_a$  are different from those in Ref. [37], which implies the LECs receive considerable corrections after we include the explicit chiral dynamics, e.g., the OPE and TPE interactions.

Then we can use the determined  $\tilde{g}_s$  and  $\tilde{g}_a$  to estimate the contact potentials of the  $\Sigma_c \Sigma_c$  systems. Their quark-level  $S$ -wave contact interactions have been systematically studied in Ref. [100], and we have

$$\mathcal{V}_{[\Sigma_c \Sigma_c]_0^0} = -\frac{20}{3}\tilde{g}_s + \frac{80}{9}\tilde{g}_a, \quad (23)$$

$$\mathcal{V}_{[\Sigma_c \Sigma_c]_0^2} = \frac{16}{3}\tilde{g}_s - \frac{64}{9}\tilde{g}_a, \quad (24)$$

$$\mathcal{V}_{[\Sigma_c \Sigma_c]_1^1} = -\frac{8}{3}\tilde{g}_s - \frac{32}{27}\tilde{g}_a. \quad (25)$$

One can obtain the LECs  $C_c$ ,  $C_d$ ,  $D_a$  and  $D_b$  through matching Eqs. (11) and (23)-(25).

TABLE III. The coefficients defined in Eq. (16) and Eq. (17) for the  $\Sigma_c \Sigma_c$  system.

	$C^{(B/R)_{i,j}}$	$C_1^{(B/R)_{i,j}}$	$C_2^{(B/R)_{i,j}}$	$C_3^{(B/R)_{i,j}}$	$C_4^{(B/R)_{i,j}}$	$C_5^{(B/R)_{i,j}}$	$\mathcal{E}_1^{(B/R)_{i,j}}$	$\mathcal{E}_2^{(B/R)_{i,j}}$
$j = 1$	$\frac{g_2^4}{4}$	-1	1/-1	1	-10	15	$\delta_b$	$\delta_b$
$j = 2, 3$	$\frac{g_1^2 g_2^2}{8}$	-1	1/-1	1	-10	15	$\delta_b$	0
$j = 4, 5$	$\frac{g_2^2 g_3^2}{24}$	-2	-1/1	2	-20	30	$\delta_b$	$-\delta_a$
$j = 6$	$\frac{g_1^4}{16}$	-1	1/-1	1	-10	15	0	0
$j = 7$	$\frac{g_3^4}{144}$	-4	1/-1	4	-40	60	$-\delta_a$	$-\delta_a$
$j = 8, 9$	$\frac{g_1^2 g_3^2}{48}$	-2	-1/1	2	-20	30	0	$-\delta_a$

In order to search for the possible bound states in the  $\Sigma_c \Sigma_c$  system via solving the Schrödinger equation, we perform the Fourier transformation on  $\mathcal{V}(\mathbf{q})$  to get the effective potential  $\mathcal{V}(r)$  in the coordinate space,

$$\mathcal{V}(r) = \int \frac{d^3 \mathbf{q}}{(2\pi)^3} e^{-i\mathbf{q}\cdot\mathbf{r}} \mathcal{V}(\mathbf{q}) \mathcal{F}(\mathbf{q}), \quad (26)$$

in which the Gaussian form factor  $\mathcal{F}(\mathbf{q}) = \exp(-\mathbf{q}^{2n}/\Lambda^{2n})$  (with  $n = 2$ ) is adopted to regularize the divergence in this integral [110, 111]. The cutoff  $\Lambda$  is introduced to exclude the hard momentum contributions.

## B. Results and discussion

In this subsection, we present the effective potentials for  $[\Sigma_c \Sigma_c]_0^{0,2}$  and  $[\Sigma_c \Sigma_c]_1^1$  systems with the cutoff and LECs in Eq. (20). We will discuss the effective potentials of the  $\Sigma_c \Sigma_c$  system in three cases.

- Case-I: We only consider the  $\Sigma_c$  as the intermediate state in the TPE diagrams.
- Case-II: We consider both the  $\Sigma_c$  and  $\Sigma_c^*$  as the intermediate states in the TPE diagrams.
- Case-III: We consider the  $\Lambda_c$ ,  $\Sigma_c$ , and  $\Sigma_c^*$  as the intermediate states in the TPE diagrams.

In Case-I, only the diagrams (F<sub>1.1</sub>), (T<sub>1.2</sub>), (T<sub>1.5</sub>), (B<sub>1.6</sub>), (R<sub>1.6</sub>) contribute. The effective potentials from the contact, OPE, and TPE interactions in coordinate space for the  $[\Sigma_c \Sigma_c]_0^0$ ,  $[\Sigma_c \Sigma_c]_1^1$ , and  $[\Sigma_c \Sigma_c]_0^2$  systems are presented in Figs. 2(a), 2(c), and 2(e), respectively. From Fig. 2(a), one sees that for the  $[\Sigma_c \Sigma_c]_0^0$  system, the TPE potential is comparable to that of OPE but with opposite sign. Consequently, the total effective potential mainly comes from the contact term, which provides a large attractive force. The contact potential of the  $[\Sigma_c \Sigma_c]_1^1$  [see Fig. 2(b)] is much smaller than that of the  $[\Sigma_c \Sigma_c]_0^0$  system. Moreover, the OPE and TPE potentials are all repulsive. Thus, the attractive force of the  $[\Sigma_c \Sigma_c]_1^1$  system is much smaller than that of the  $[\Sigma_c \Sigma_c]_0^0$  system.

In Figs. 2(b), 2(d), and 2(f), we present the contributions of each type of the TPE diagrams in momentum space. The  $\mathcal{V}_{1\text{Itm}}^{\Sigma_c}$  and  $\mathcal{V}_{1\text{Itm}}^{\Sigma_c \Sigma_c}$  denote  $\mathcal{V}_{1\text{Itm}}^{\Sigma_c} = \mathcal{V}^{\text{T}_{1.2}} + \mathcal{V}^{\text{T}_{1.5}}$ , and  $\mathcal{V}_{1\text{Itm}}^{\Sigma_c \Sigma_c} = \mathcal{V}^{\text{B}_{1.6}} + \mathcal{V}^{\text{R}_{1.6}}$ . The positive (negative) effective potential in

momentum space corresponds to a repulsive (attractive) force in coordinate space. From Figs. 2(b) and 2(f), one sees that the contributions of (B<sub>1.6</sub>) and (R<sub>1.6</sub>) are considerable but with opposite signs. Thus, the sum of these two potentials give a relatively small  $\mathcal{V}_{1\text{Itm}}^{\Sigma_c \Sigma_c}$ . As collected in Table II, the isospin factor  $F_1^{\text{R}_{1.6}}$  vanishes for the  $[\Sigma_c \Sigma_c]_1^1$  system. Thus, we have  $\mathcal{V}_{1\text{Itm}}^{\Sigma_c \Sigma_c} = \mathcal{V}^{\text{B}_{1.6}}$ , as presented in Fig. 2(d). Besides, the magnitudes of the TPE diagrams are comparable to each other for the  $[\Sigma_c \Sigma_c]_0^{0,2}$  and  $[\Sigma_c \Sigma_c]_1^1$  systems.

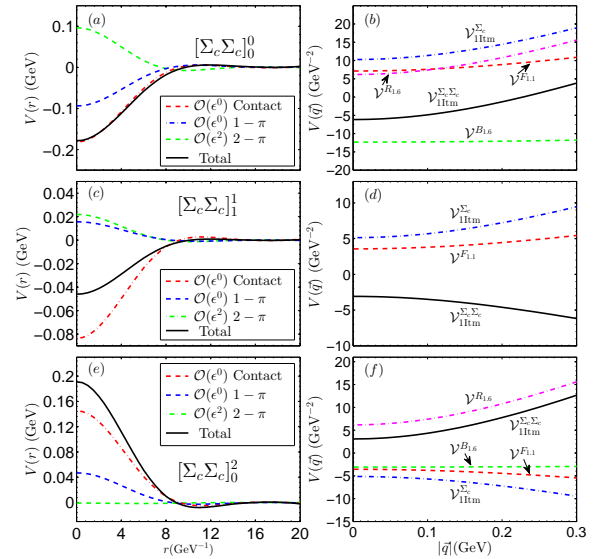


FIG. 2. The first, second, and third rows are the effective potentials of the  $[\Sigma_c \Sigma_c]_0^0$ ,  $[\Sigma_c \Sigma_c]_1^1$ , and  $[\Sigma_c \Sigma_c]_0^2$  systems, respectively. The  $\mathcal{V}_{1\text{Itm}}^{\Sigma_c}$  and  $\mathcal{V}_{1\text{Itm}}^{\Sigma_c \Sigma_c}$  are defined as  $\mathcal{V}_{1\text{Itm}}^{\Sigma_c} = \mathcal{V}^{\text{T}_{1.2}} + \mathcal{V}^{\text{T}_{1.5}}$  and  $\mathcal{V}_{1\text{Itm}}^{\Sigma_c \Sigma_c} = \mathcal{V}^{\text{B}_{1.6}} + \mathcal{V}^{\text{R}_{1.6}}$ , respectively.

In the heavy quark limit, the  $\Sigma_c$  and  $\Sigma_c^*$  baryons are degenerate. In order to evaluate the contributions of the TPE diagrams, we divide the Case-II into two scenarios—without and with considering the mass difference  $\delta_a$  between the intermediate  $\Sigma_c^*$  and initial  $\Sigma_c$  baryon. We present the effective potentials with  $\delta_a = 0$  for the  $[\Sigma_c \Sigma_c]_0^{0,2}$  and  $[\Sigma_c \Sigma_c]_1^1$  systems in Fig. 3. In Figs. 3(a), 3(d), and 3(g), the inclusion of  $\Sigma_c^*$ -related channels gives minor corrections to the TPE potentials of the  $\Sigma_c \Sigma_c$  systems. The contributions of the triangle diagrams with the  $\Sigma_c^*$  as the intermediate state is slightly smaller

than that of triangle diagrams with the  $\Sigma_c$  as the intermediate state, as can be seen from Figs. 3(b), 3(e), and 3(h). The contributions of the box plus cross diagrams with the  $\Sigma_c\Sigma_c$  and  $\Sigma_c\Sigma_c^*$  as the intermediate channels are comparable to each other, and are bigger than that of the box plus cross diagrams with the  $\Sigma_c^*\Sigma_c^*$  as the intermediate channels.

Then we discuss the scenario of considering the mass splitting  $\delta_a$  in the TPE diagrams. In this scenario, we still have the relation

$$|\mathcal{V}_{1\text{Itm}}^{\Sigma_c}| > |\mathcal{V}_{1\text{Itm}}^{\Sigma_c^*}| \quad (27)$$

for the triangle diagrams. However, for the box plus cross diagrams, we obtain the following relation

$$|\mathcal{V}_{1\text{Itm}}^{\Sigma_c\Sigma_c}| \approx |\mathcal{V}_{1\text{Itm}}^{\Sigma_c^*\Sigma_c^*}| < |\mathcal{V}_{1\text{Itm}}^{\Sigma_c\Sigma_c^*}|, \quad (28)$$

i.e., the contributions of the box plus cross diagrams with the  $\Sigma_c^*\Sigma_c^*$  as the intermediate state are comparable to that of the box plus cross diagrams with the  $\Sigma_c\Sigma_c$  as intermediate state and are much smaller than that of the box plus cross diagrams with the  $\Sigma_c\Sigma_c^*$  as the intermediate state. In this scenario, the  $[\Sigma_c\Sigma_c]_0^{0,2}$  and  $[\Sigma_c\Sigma_c]_1^1$  are all deeply bound (the binding energies are all larger than 100 MeV). The main reason of the unnaturally large binding energies is that we used the dimensional regulation scheme to calculate the TPE loop diagrams. The chiral loops calculated with this regulation scheme will lead to convergence problems [112–114]. The results of including the mass splittings might be uncontrollable in the present dimensional regulation scheme. Thus, in the following, we only present the results without the mass differences in the TPE potentials.

The mass difference  $\delta_b$  ( $\delta_c$ ) between the  $\Lambda_c$  and  $\Sigma_c^{(*)}$  baryons are from that of the scalar and vector diquarks inside the  $\Lambda_c$  and  $\Sigma_c^{(*)}$  baryons. However, if we take these mass differences into account, we have to face the above mentioned convergence problem again. To roughly estimate the effects of including the  $\Lambda_c$ -related channels, we will not consider the mass differences  $\delta_b$  and  $\delta_c$  in the TPE potentials. The results in Case-III for the  $[\Sigma_c\Sigma_c]_0^{0,2}$ ,  $[\Sigma_c\Sigma_c]_1^1$  systems are presented in Fig. 4. One sees that including the  $\Lambda_c$ -related intermediate channels can give very important corrections to the TPE potentials, and the relative contributions of the intermediate channels roughly have the following relations

$$|\mathcal{V}_{1\text{Itm}}^{\Sigma_c}| > |\mathcal{V}_{1\text{Itm}}^{\Lambda_c}| > |\mathcal{V}_{1\text{Itm}}^{\Sigma_c^*}|, \quad (29)$$

$$|\mathcal{V}_{1\text{Itm}}^{\Lambda_c\Sigma_c}| > |\mathcal{V}_{1\text{Itm}}^{\Lambda_c\Lambda_c}| \approx |\mathcal{V}_{1\text{Itm}}^{\Lambda_c\Sigma_c^*}|, \quad (30)$$

$$|\mathcal{V}_{1\text{Itm}}^{\Sigma_c\Sigma_c}| \approx |\mathcal{V}_{1\text{Itm}}^{\Sigma_c^*\Sigma_c^*}| > |\mathcal{V}_{1\text{Itm}}^{\Sigma_c\Sigma_c^*}|. \quad (31)$$

The above relations are consistent with the general understanding of the couple-channel effect.

The total effective potentials of the  $[\Sigma_c\Sigma_c]_0^0$  and  $[\Sigma_c\Sigma_c]_1^1$  are both attractive and can form bound states. The corresponding binding energies are 101.9 MeV and 6.8 MeV, respectively. Since the width of the  $\Sigma_c^+$  baryon is about 2 MeV and its dominant decay mode is  $\Sigma_c^+ \rightarrow \Lambda_c^+\pi^0$  [5]. Thus, these two bound states are expected to be narrow. One may find the  $[\Sigma_c\Sigma_c]_0^0$  bound state in the  $\Lambda_c\Lambda_c$  invariant mass distributions.

For the shallow bound state  $[\Sigma_c\Sigma_c]_1^1$ , it can be detected in the  $\Lambda_c\pi\Lambda_c\pi$  and  $\Lambda_c\Lambda_c\pi$  final states.

With the same framework, we further study the interactions of the  $\Lambda_c\Lambda_c$  and  $\Lambda_c\Sigma_c$  systems. The symmetry allowed systems are  $[\Lambda_c\Lambda_c]_0^0$  and  $[\Lambda_c\Sigma_c]_{0,1}^1$ . We present our results for these two systems in Appendix A.

## IV. SUMMARY

In this work, we have studied the interactions of the  $\Sigma_c\Sigma_c$  systems within  $\chi$ EFT. We introduce the contact, OPE, and TPE interactions for the  $[\Sigma_c\Sigma_c]_0^{0,2}$  and  $[\Sigma_c\Sigma_c]_1^1$  systems and determine the LECs from the  $\Sigma_c^{(*)}\bar{D}^{(*)}$  systems via a quark-level interaction.

We explore the effects of different intermediate channels in the TPE diagrams in three cases. We introduce the (i)  $\Sigma_c$ , (ii)  $\Sigma_c, \Sigma_c^*$  and (iii)  $\Lambda_c, \Sigma_c, \Sigma_c^*$  as the possible intermediate states gradually. We find the convergence of the chiral expansion is not good if the mass splittings are explicitly considered in the TPE potentials within the dimensional regularization scheme, which results in deeply bound molecular states with unnaturally large binding energies. To cure this problem, we neglect the mass differences between the initial  $\Sigma_c$  and intermediate ( $\Lambda_c, \Sigma_c, \Sigma_c^*$ ) baryons. In this case, the interactions of the  $[\Sigma_c\Sigma_c]_0^0$  and  $[\Sigma_c\Sigma_c]_1^1$  are attractive, while the interaction of the  $[\Sigma_c\Sigma_c]_0^2$  system is repulsive. Among the three cases, the TPE potentials in Case-II are very close to that of Case-I, and the NLO TPE potentials are comparable to the LO OPE potentials. But if we include the  $\Lambda_c$  as the intermediate channels, the TPE potentials for the  $[\Sigma_c\Sigma_c]_1^1$  and  $[\Sigma_c\Sigma_c]_0^2$  change their signs and the power counting works well.

We obtain two bound states in the  $\Sigma_c\Sigma_c$  systems—the  $[\Sigma_c\Sigma_c]_0^0$  and  $[\Sigma_c\Sigma_c]_1^1$ . These two states should be narrow ones due to the small width of the  $\Sigma_c$  baryon. The  $[\Sigma_c\Sigma_c]_0^0$  and  $[\Sigma_c\Sigma_c]_1^1$  may be reconstructed in the  $\Lambda_c\Lambda_c$  and  $(\Lambda_c^+\pi\Lambda_c^+\pi, \Lambda_c^+\Lambda_c^+\pi)$  final states, respectively. We hope that the experiments at LHC, J-PARC, and RHIC can search for these two states in the future.

## ACKNOWLEDGMENTS

This work is supported by the National Natural Science Foundation of China under Grants No. 11975033, No. 12105072 and No. 12070131001, the Youth Funds of Hebei Province (No. A2021201027) and the Start-up Funds for Young Talents of Hebei University (No. 521100221021).

### Appendix A: The interactions of the $\Lambda_c\Lambda_c$ and $\Lambda_c\Sigma_c$ systems

#### 1. The effective potentials for the $\Lambda_c\Lambda_c$ and $\Lambda_c\Sigma_c$ systems

Since the vertex  $\Lambda_c\Lambda_c\pi$  does not exist, there is no OPE contribution in the  $\Lambda_c\Lambda_c$  system. The contact potential reads

$$\mathcal{V}_{\Lambda_c\Lambda_c}^{\text{ct}} = -16C_a. \quad (\text{A1})$$

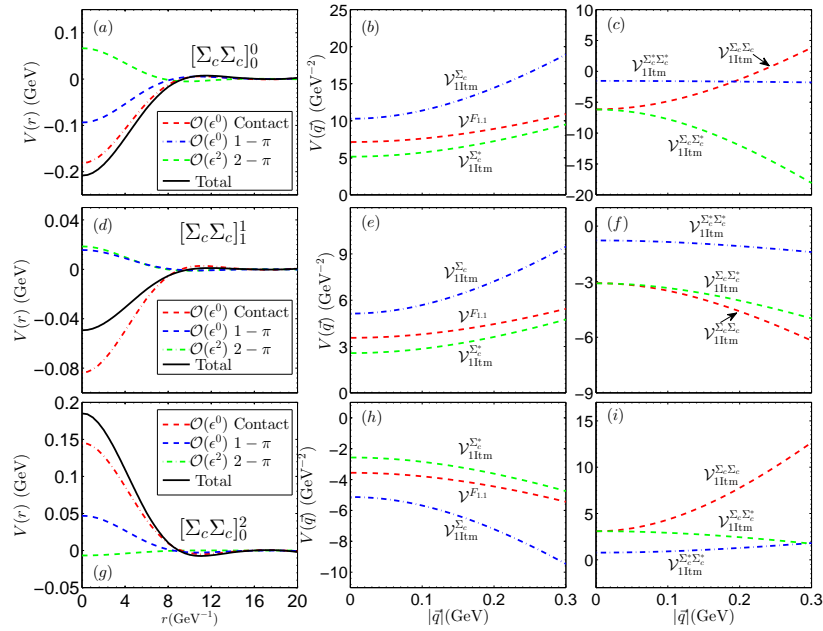


FIG. 3. The first, second, and third rows are the effective potentials of the  $[\Sigma_c \Sigma_c]_0^0$ ,  $[\Sigma_c \Sigma_c]_1^1$ , and  $[\Sigma_c \Sigma_c]_0^2$  systems, respectively. The  $\mathcal{V}_{1ltm}^{\Sigma_c^*}$ ,  $\mathcal{V}_{1ltm}^{\Sigma_c \Sigma_c^*}$  and  $\mathcal{V}_{1ltm}^{\Sigma_c^* \Sigma_c^*}$  are the results of the  $\mathcal{V}^{T_{1.3}} + \mathcal{V}^{T_{1.6}}$ ,  $\mathcal{V}^{B_{1.8}} + \mathcal{V}^{B_{1.9}} + \mathcal{V}^{R_{1.8}} + \mathcal{V}^{R_{1.9}}$ , and  $\mathcal{V}^{B_{1.7}} + \mathcal{V}^{R_{1.7}}$  in momentum space, respectively. The other notations are the same as in Fig. 2.

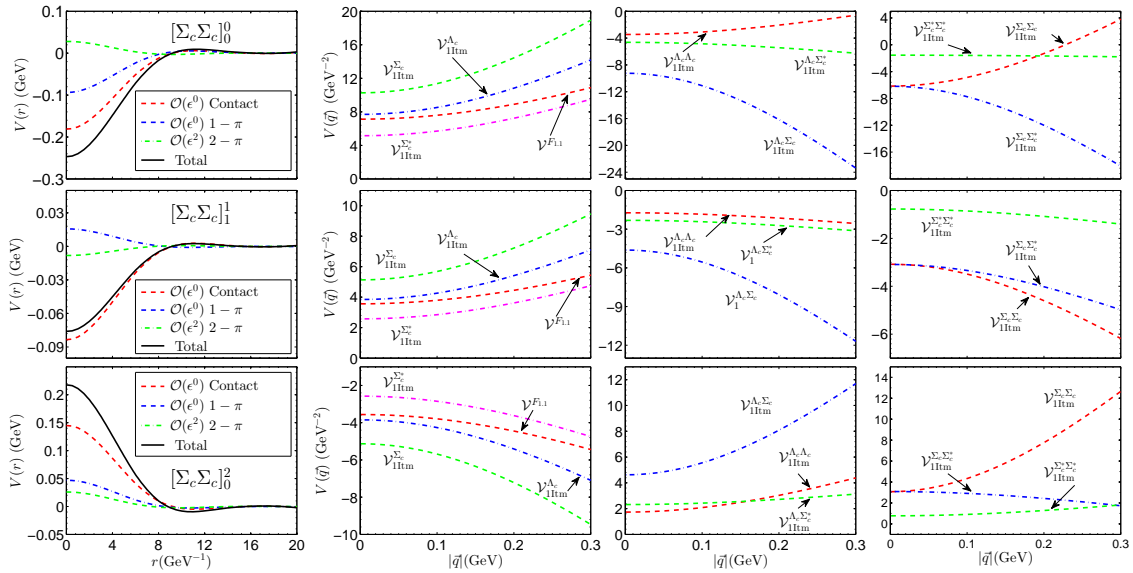


FIG. 4. The first, second, and third rows are the effective potentials of the  $[\Lambda_c \Sigma_c]_0^0$ ,  $[\Lambda_c \Sigma_c]_1^1$ , and  $[\Lambda_c \Sigma_c]_0^2$  systems, respectively. The  $\mathcal{V}_{1ltm}^{\Lambda_c}$ ,  $\mathcal{V}_{1ltm}^{\Lambda_c \Lambda_c}$ ,  $\mathcal{V}_{1ltm}^{\Lambda_c \Sigma_c}$ , and  $\mathcal{V}_{1ltm}^{\Lambda_c \Sigma_c^*}$  are the results of the  $\mathcal{V}^{T_{1.1}} + \mathcal{V}^{T_{1.4}}$ ,  $\mathcal{V}^{B_{1.1}} + \mathcal{V}^{R_{1.1}}$ ,  $\mathcal{V}^{B_{1.2}} + \mathcal{V}^{R_{1.2}} + \mathcal{V}^{B_{1.3}} + \mathcal{V}^{R_{1.3}}$ , and  $\mathcal{V}^{B_{1.4}} + \mathcal{V}^{R_{1.4}} + \mathcal{V}^{B_{1.5}} + \mathcal{V}^{R_{1.5}}$  in momentum space, respectively. The other notations are the same as in Fig. 2 and Fig. 3.

Because the  $\Lambda_c$  baryon has a spin-0 diquark, the spin-spin interaction from the light degree of freedom vanishes and only the central interaction term survives.

For the  $\Lambda_c \Sigma_c$  system, the corresponding contact and OPE potentials read

$$\mathcal{V}_{\Lambda_c \Sigma_c}^{\text{ct}} = 2C_b, \quad (\text{A2})$$

$$\mathcal{V}_{\Lambda_c \Sigma_c}^{\text{OPE}} = -\frac{g_2^2}{2f_\pi^2} \frac{(\boldsymbol{\sigma}_1 \cdot \mathbf{q})(\boldsymbol{\sigma}_2 \cdot \mathbf{q})}{q^2 + m_\pi^2}. \quad (\text{A3})$$

From Eq. (A2), the contact potentials of the  $[\Lambda_c \Sigma_c]_0^1$  and  $[\Lambda_c \Sigma_c]_1^1$  states are the same. The differences between the effective potentials of these two states will be manifested in their OPE and TPE potentials.

The TPE diagrams for the  $\Lambda_c \Lambda_c$  and  $\Lambda_c \Sigma_c$  systems are pre-

sented in Fig. 5 and Fig. 6, respectively. Since the  $\Lambda_c \Lambda_c \pi \pi$  vertex does not exist, the  $\Lambda_c \Lambda_c$  system does not have the football or triangle diagrams. Since the  $\Lambda_c \Lambda_c \pi$  vertex is forbidden, as presented in Fig. 5, the intermediate channels for the  $\Lambda_c \Lambda_c$  system can only be the  $\Sigma_c \Sigma_c$ ,  $\Sigma_c \Sigma_c^*$ , and  $\Sigma_c^* \Sigma_c^*$  in the box diagrams  $B_{2,1} - B_{2,4}$  and cross diagrams  $R_{2,1} - R_{2,4}$ .

Similar to the  $\Lambda_c \Lambda_c$  system, the  $\Lambda_c \Sigma_c$  system does not have the football diagram. The obtained amplitudes of the triangle diagrams for the  $\Lambda_c \Sigma_c$  system vanish. Thus, we do not depict them in Fig. 6. The box diagrams  $B_{3,1} - B_{3,9}$  and cross diagrams  $R_{3,1} - R_{3,9}$  with the final states unchanged  $(B/R)_{3,1} - (B/R)_{3,6}$  and interchanged  $(B/R)_{3,7} - (B/R)_{3,9}$  are depicted in Fig. 6.

The expressions of the box and cross diagrams for the  $\Lambda_c \Lambda_c$  and  $\Lambda_c \Sigma_c$  systems can also be expressed as Eq. (16) and Eq. (17), respectively. Note that the  $\Lambda_c \Lambda_c$  and  $\Lambda_c \Sigma_c$  can only couple to the isospin 0 and 1 states, respectively. Thus, the isospin factors  $F_I^{B_{i,j}}$  ( $F_I^{R_{i,j}}$ ) defined in Eq. (16) (Eq. (17)) are just 1 for each of the box (cross) diagrams in the  $\Lambda_c \Lambda_c$  and  $\Lambda_c \Sigma_c$  systems. The other coefficients defined in Eq. (16) and Eq. (17) are collected in Table IV.

## 2. Results and discussion

The leading order contact terms for the  $[\Lambda_c \Lambda_c]_0^0$  and  $[\Lambda_c \Sigma_c]_{0,1}^1$  systems at quark level [100] are

$$\begin{aligned} \mathcal{V}_{[\Lambda_c \Lambda_c]_0^0} &= \frac{4}{3} \tilde{g}_s, \\ \mathcal{V}_{[\Lambda_c \Sigma_c]_{0,1}^1} &= \frac{4}{3} \tilde{g}_s. \end{aligned}$$

Correspondingly, we obtain the LECs defined in Eq. 7 as

$$C_a = -1.3 \text{ GeV}^{-2}, \quad C_b = 10.4 \text{ GeV}^{-2}. \quad (\text{A4})$$

With the above preparation, we calculate the total effective potentials for the  $[\Lambda_c \Lambda_c]_0^0$  and  $[\Lambda_c \Sigma_c]_{0,1}^1$  systems. Then we solve the corresponding Schrödinger equations to search for the binding solutions.

We first present the results of the  $\Lambda_c \Lambda_c$  system. To calculate the two-pion-exchange effective potential, we firstly neglect the mass differences between the intermediate  $\Sigma_c^{(*)} \Sigma_c^{(*)}$  channels with the initial  $\Lambda_c \Lambda_c$  state, i.e., we set  $\delta_b = \delta_c = 0$ . Correspondingly, we need to adopt

$$J_{ab}^B(0,0) = \frac{\partial}{\partial x} J_{ab}^T(x) \Big|_{x \rightarrow 0}, \quad (\text{A5})$$

$$J_{ab}^R(0,0) = -\frac{\partial}{\partial x} J_{ab}^T(x) \Big|_{x \rightarrow 0} \quad (\text{A6})$$

to replace the scalar loop functions in Eq. (16-17).

In Fig. 7 (a), we present the contact, two-pion-exchange, and total effective potentials of the  $[\Lambda_c \Lambda_c]_0^0$  systems in coordinate space. As illustrated in Fig. 7 (a), the contact and two-pion-exchange potentials provide the repulsive and positive forces, respectively. Besides, the contact potential is comparable to the two-pion-exchange potential but with the opposite sign. Note that the determined contact interaction is indeed a

small repulsive force due to the weak couplings between the two  $\Lambda_c$  baryons with spin-0 diquarks. Thus, the total effective potential of the  $[\Lambda_c \Lambda_c]_0^0$  system is very weak. Of course, the obtained potential can not form a  $[\Lambda_c \Lambda_c]_0^0$  bound state.

Since the magnitude of the contributions from the two-pion-exchange diagrams is comparable to that of the contact term, we further check the relative contributions of the intermediate  $\Sigma_c^{(*)} \Sigma_c^{(*)}$  channels in the  $\Lambda_c \Lambda_c$  system. In momentum space, we present the effective potentials of the  $(B_{2,1}, R_{2,1})$ ,  $(B_{2,2} + B_{2,3}, R_{2,2} + R_{2,3})$ , and  $(B_{2,4}, R_{2,4})$  diagrams in Fig. 7 (b), (c), and (d), respectively. From Fig. 7 (b), we can easily find out that the  $B_{2,1}$  and  $R_{2,1}$  provide the attractive and repulsive forces, respectively. We also sum the  $\mathcal{V}^{B_{2,1}}$  and  $\mathcal{V}^{R_{2,1}}$  to give the total potential induced from including the  $\Sigma_c \Sigma_c$  intermediate channel. Summing the  $V^{B_{2,2}} + V^{B_{2,3}}$  and  $V^{R_{2,2}} + V^{R_{2,3}}$ , we find that the inclusion of the  $\Sigma_c \Sigma_c^*$  channel provides a repulsive force to the  $\Lambda_c \Lambda_c$  system, and this channel is more important than the  $\Sigma_c \Sigma_c$  intermediate channel. Besides, as can be seen from Fig. 7 (d), the  $\Sigma_c^* \Sigma_c^*$  channel gives very tiny contribution to the two-pion-exchange potential. Although the contributions of the  $V^{B_{2,4}}$  and  $V^{R_{2,4}}$  are considerable, their opposite signs make the  $V_{21\text{tm}}^{\Sigma_c^* \Sigma_c^*}$  negligible.

We further check the results of the  $[\Lambda_c \Lambda_c]_0^0$  by including the mass differences between the initial  $\Lambda_c$  and the intermediate  $\Sigma_c / \Sigma_c^*$  states. However, we find that the convergence of the chiral series problem also exists in the  $\Lambda_c \Lambda_c$  system. After considering the mass differences, the contributions from the two-pion-exchange diagrams are significantly magnified. The obtained two-pion-exchange potential is much larger than the leading order contact potential, which may violate the power counting rule. The unexpected total large potential will lead to a very deeply bound state with the binding energy 197 MeV.

We also check the relative contributions from the intermediate  $\Sigma_c \Sigma_c$ ,  $\Sigma_c \Sigma_c^*$ , and  $\Sigma_c^* \Sigma_c^*$  channels. After we include the mass differences, these three channels all provide strong attractive forces and have

$$\left| \mathcal{V}_{11\text{tm}}^{\Sigma_c \Sigma_c} \right| < \left| \mathcal{V}_{11\text{tm}}^{\Sigma_c \Sigma_c^*} \right| < \left| \mathcal{V}_{11\text{tm}}^{\Sigma_c^* \Sigma_c^*} \right|. \quad (\text{A7})$$

Generally, the intermediate channel would have less influence to the studied two-body system if its threshold lies further away from the threshold of the considered system. The obtained results contradicts this argument. The  $[\Lambda_c \Sigma_c]_{0,1}^1$  have very similar results due to the uncertainties introduced from the nonanalytic chiral loops in the two-pion-exchange loop diagrams. Thus, in the following, we only discuss the  $\Lambda_c \Sigma_c$  system without considering the mass differences between the initial and intermediate baryons, i.e., we adopt  $\delta_a = \delta_b = \delta_c$ .

The effective potentials of the  $[\Lambda_c \Sigma_c]_{0,1}^1$  system are presented in Fig. 8. The leading order contact potentials of the  $[\Lambda_c \Sigma_c]_{0,1}^1$  systems arise from the interactions of their light degrees of freedom (d.o.f). The  $[\Lambda_c \Sigma_c]_0^1$  and  $[\Lambda_c \Sigma_c]_1^1$  have the same contact potentials. The corrections from the spin of heavy quarks are manifest after we include the one-pion-exchange and two-pion-exchange interactions. As presented in Fig. 8 (a) and (d), the one-pion-exchange potentials provide the repulsive and attractive forces in the  $[\Lambda_c \Sigma_c]_0^1$  and  $[\Lambda_c \Sigma_c]_1^1$  systems, respectively. In both systems, the magnitudes of the

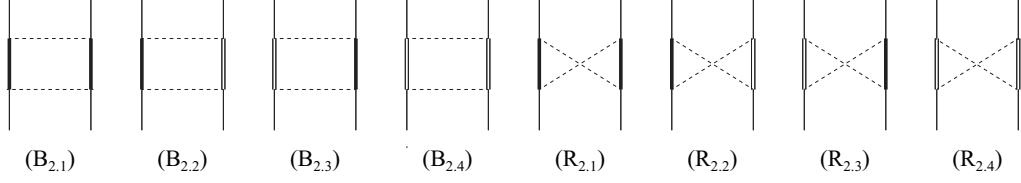


FIG. 5. Two-pion-exchange diagrams that account for the effective potentials of the  $\Lambda_c \Lambda_c$  system at next-to-leading order. These diagrams include the box diagram ( $B_{2,i}$ ) and cross diagram ( $R_{2,i}$ ). We use the thin line, thick line, double-thin line, and dashed line to denote the  $\Lambda_c$ ,  $\Sigma_c$ ,  $\Sigma_c^*$ , and  $\pi$ , respectively.

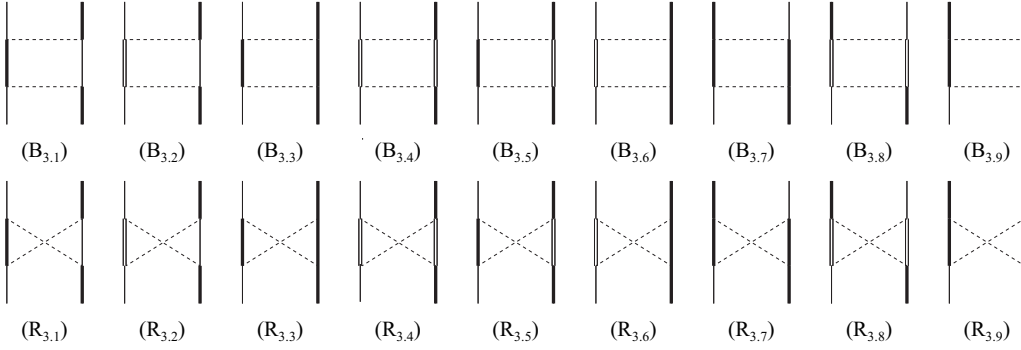


FIG. 6. Two-pion-exchange diagrams for the  $\Lambda_c \Sigma_c$  system. The notations are the same as those in Fig. 5

TABLE IV. The coefficients of the two-pion-exchange box and cross diagrams defined in Eq. (16) and Eq. (17) for the  $\Lambda_c \Lambda_c$  and  $\Lambda_c \Sigma_c$  systems.

	$C^{(B/R)_{i,j}}$	$C_1^{(B/R)_{i,j}}$	$C_2^{(B/R)_{i,j}}$	$C_3^{(B/R)_{i,j}}$	$C_4^{(B/R)_{i,j}}$	$C_5^{(B/R)_{i,j}}$	$\mathcal{E}_1^{(B/R)_{i,j}}$	$\mathcal{E}_2^{(B/R)_{i,j}}$	
$i = 2$	$j = 1$	$\frac{3g_2^4}{4}$	-1	1/-1	1	-10	15	$-\delta_b$	$-\delta_b$
	$j = 2, 3$	$\frac{g_2^2 g_4^2}{4}$	-2	-1/1	2	-20	30	$-\delta_b$	$-\delta_c$
	$j = 4$	$\frac{g_4^4}{12}$	-4	1/-1	4	-40	60	$-\delta_c$	$-\delta_c$
$i = 3$	$j = 1$	$\frac{g_2^4}{4}$	-1	1/-1	1	-10	15	$\delta_b$	$-\delta_b$
	$j = 2$	$\frac{g_2^2 g_4^2}{12}$	-2	-1/1	2	-20	30	$\delta_b$	$-\delta_c$
	$j = 3$	$\frac{g_1^2 g_2^2}{4}$	-1	1/-1	1	-10	15	0	$-\delta_b$
	$j = 4$	$\frac{g_3^2 g_4^2}{36}$	-4	1/-1	4	-40	60	$-\delta_a$	$-\delta_c$
	$j = 5$	$\frac{g_2^2 g_3^2}{12}$	-2	-1/1	2	-20	30	$-\delta_a$	$-\delta_b$
	$j = 6$	$\frac{g_1^2 g_4^2}{12}$	-2	-1/1	2	-20	30	0	$-\delta_c$
	$j = 7$	$\frac{g_1^2 g_2^2}{4}$	1/-1	-1	-1/1	10/-10	-15/15	0	$-\delta_b$
	$j = 8$	$\frac{g_3^2 g_4^2}{36}$	4/-4	-1	-4/4	40/-40	-60/60	$-\delta_a$	$-\delta_c$
	$j = 9$	$\frac{g_1 g_2 g_3 g_4}{6}$	2/-2	1	-2/2	20/-20	-30/30	$-\delta_a$	$-\delta_b$

one-pion-exchange and contact contributions are comparable to each other and much smaller than those of the two-pion-exchange potentials. Note that the contact interaction for the  $\Lambda_c \Sigma_c$  system determined from quark model is identical to that of the  $\Lambda_c \Lambda_c$  system. Thus, the contact interactions of the

$[\Lambda_c \Sigma_c]_{0,1}^1$  systems are relatively small. For such a system, it is very likely that their two-pion-exchange potentials are larger than its contact term.

We further check the relative contributions from different intermediate channels. We present the effective potentials in-

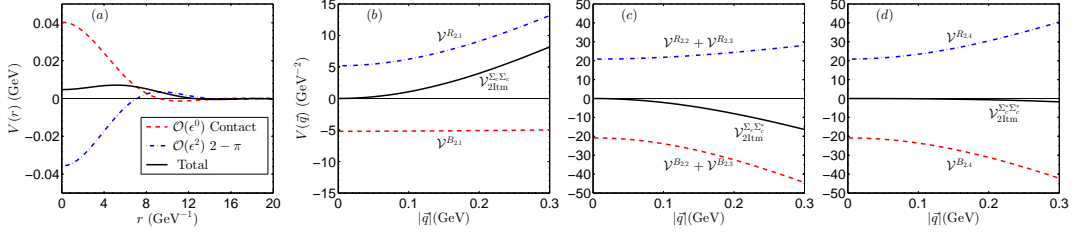


FIG. 7. (a) present the contact, TPE, and total effective potentials of the  $[\Lambda_c \Lambda_c]_0^0$  system in the coordinate space. (b), (c), and (d) depict the contributions of two-pion-exchange diagrams in momentum space. The  $\mathcal{V}_{2\text{I}tm}^{\Sigma_c \Sigma_c^*}$ ,  $\mathcal{V}_{2\text{I}tm}^{\Sigma_c \Sigma_c^*}$ , and  $\mathcal{V}_{2\text{I}tm}^{\Sigma_c^* \Sigma_c^*}$  are the results of  $\mathcal{V}^{B_{2.1}} + \mathcal{V}^{R_{2.1}}$ ,  $\mathcal{V}^{B_{2.2}} + \mathcal{V}^{B_{2.3}} + \mathcal{V}^{R_{2.2}} + \mathcal{V}^{R_{2.3}}$ , and  $\mathcal{V}^{B_{2.4}} + \mathcal{V}^{R_{2.4}}$  that account for the contributions induced from including the  $\Sigma_c \Sigma_c$ ,  $\Sigma_c \Sigma_c^*$ , and  $\Sigma_c^* \Sigma_c^*$  intermediate channels, respectively.

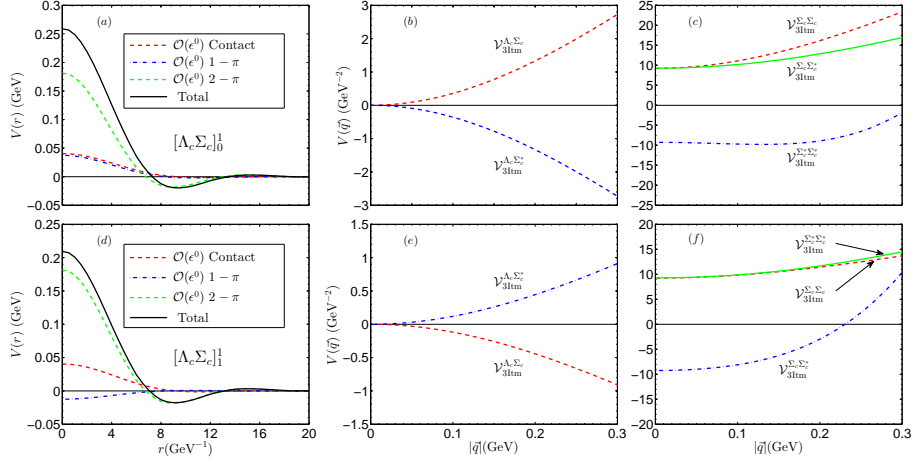


FIG. 8. (a) and (d) present the contact, OPE, TPE, and total effective potentials of the  $[\Lambda_c \Sigma_c]_0^0$  system in the coordinate space. (b), (c), (e) (f) depict the contributions of two-pion-exchange diagrams. The  $\mathcal{V}_{3\text{I}tm}^{\Lambda_c \Sigma_c}$ ,  $\mathcal{V}_{3\text{I}tm}^{\Lambda_c \Sigma_c^*}$ ,  $\mathcal{V}_{3\text{I}tm}^{\Sigma_c \Sigma_c}$ ,  $\mathcal{V}_{3\text{I}tm}^{\Sigma_c \Sigma_c^*}$ , and  $\mathcal{V}_{3\text{I}tm}^{\Sigma_c^* \Sigma_c^*}$  are the results of  $\mathcal{V}^{B_{3.1}} + \mathcal{V}^{R_{3.1}}$ ,  $\mathcal{V}^{B_{3.2}} + \mathcal{V}^{R_{3.2}}$ ,  $\mathcal{V}^{B_{3.3}} + \mathcal{V}^{R_{3.3}} + \mathcal{V}^{B_{3.7}} + \mathcal{V}^{R_{3.7}}$ ,  $\mathcal{V}^{B_{3.5}} + \mathcal{V}^{R_{3.5}} + \mathcal{V}^{B_{3.6}} + \mathcal{V}^{R_{3.6}} + \mathcal{V}^{B_{3.9}} + \mathcal{V}^{R_{3.9}}$ , and  $\mathcal{V}^{B_{3.4}} + \mathcal{V}^{R_{3.4}} + \mathcal{V}^{B_{3.8}} + \mathcal{V}^{R_{3.8}}$  that account for the contributions induced from including the  $\Lambda_c \Sigma_c$ ,  $\Lambda_c \Sigma_c^*$ ,  $\Sigma_c \Sigma_c$ ,  $\Sigma_c \Sigma_c^*$ , and  $\Sigma_c^* \Sigma_c^*$  intermediate channels, respectively.

duced from the intermediate  $\Lambda_c \Sigma_c^{(*)}$  and  $\Sigma_c^{(*)} \Sigma_c^{(*)}$  channels in momentum space in Fig. 8 (b), (c), (e), and (f). The  $\Lambda_c \Sigma_c$  and  $\Lambda_c \Sigma_c^*$  have relatively small contributions to the two-

pion-exchange potential, while the contributions of the  $\Sigma_c \Sigma_c$ ,  $\Sigma_c \Sigma_c^*$  and  $\Sigma_c^* \Sigma_c^*$  channels are comparable to each other and quite important.

- 
- [1] S. Godfrey and N. Isgur, *Phys. Rev. D* **32** (1985), 189-231  
[2] S. Capstick and N. Isgur, *AIP Conf. Proc.* **132** (1985), 267-271  
[3] B. Aubert *et al.* [BaBar], *Phys. Rev. Lett.* **90** (2003), 242001  
[4] S. K. Choi *et al.* [Belle], *Phys. Rev. Lett.* **91** (2003), 262001  
[5] P. A. Zyla *et al.* [Particle Data Group], *PTEP* **2020**, no.8, 083C01 (2020).  
[6] H. X. Chen, W. Chen, X. Liu and S. L. Zhu, *Phys. Rept.* **639**, 1-121 (2016)  
[7] Y. R. Liu, H. X. Chen, W. Chen, X. Liu and S. L. Zhu, *Prog. Part. Nucl. Phys.* **107**, 237-320 (2019)  
[8] X. Liu, *Chin. Sci. Bull.* **59**, 3815-3830 (2014)  
[9] F. K. Guo, C. Hanhart, U. G. Meißner, Q. Wang, Q. Zhao and B. S. Zou, *Rev. Mod. Phys.* **90**, no.1, 015004 (2018)  
[10] A. Hosaka, T. Iijima, K. Miyabayashi, Y. Sakai and S. Yasui, *PTEP* **2016**, no.6, 062C01 (2016)  
[11] R. F. Lebed, R. E. Mitchell and E. S. Swanson, *Prog. Part. Nucl. Phys.* **93**, 143-194 (2017)  
[12] A. Esposito, A. Pilloni and A. D. Polosa, *Phys. Rept.* **668**, 1-97 (2017)  
[13] N. Brambilla, S. Eidelman, C. Hanhart, A. Nefediev, C. P. Shen, C. E. Thomas, A. Vairo and C. Z. Yuan, *Phys. Rept.* **873**, 1-154 (2020)  
[14] H. X. Chen, W. Chen, X. Liu, Y. R. Liu and S. L. Zhu, [arXiv:2204.02649 [hep-ph]].  
[15] L. Meng, B. Wang, G. J. Wang and S. L. Zhu, arXiv:2204.08716 [hep-ph].  
[16] R. Aaij *et al.* [LHCb Collaboration], *Phys. Rev. Lett.* **115**, 072001 (2015).  
[17] R. Aaij *et al.* [LHCb Collaboration], *Phys. Rev. Lett.* **117**, no. 8, 082002 (2016).

- [18] R. Aaij *et al.* [LHCb Collaboration], *Phys. Rev. Lett.* **122**, no. 22, 222001 (2019).
- [19] J. J. Wu, R. Molina, E. Oset and B. S. Zou, *Phys. Rev. Lett.* **105**, 232001 (2010)
- [20] Z. C. Yang, Z. F. Sun, J. He, X. Liu and S. L. Zhu, *Chin. Phys. C* **36**, 6-13 (2012)
- [21] W. L. Wang, F. Huang, Z. Y. Zhang and B. S. Zou, *Phys. Rev. C* **84**, 015203 (2011)
- [22] R. Chen, Z. F. Sun, X. Liu and S. L. Zhu, *Phys. Rev. D* **100**, no.1, 011502 (2019)
- [23] M. Z. Liu, Y. W. Pan, F. Z. Peng, M. Sánchez Sánchez, L. S. Geng, A. Hosaka and M. Pavon Valderrama, *Phys. Rev. Lett.* **122**, no.24, 242001 (2019)
- [24] J. He, *Eur. Phys. J. C* **79**, no.5, 393 (2019)
- [25] C. W. Xiao, J. Nieves and E. Oset, *Phys. Rev. D* **100**, no.1, 014021 (2019)
- [26] L. Meng, B. Wang, G. J. Wang and S. L. Zhu, *Phys. Rev. D* **100**, no.1, 014031 (2019)
- [27] Y. Yamaguchi, H. García-Tecocoatzi, A. Giachino, A. Hosaka, E. Santopinto, S. Takeuchi and M. Takizawa, *Phys. Rev. D* **101**, no.9, 091502 (2020)
- [28] M. Pavon Valderrama, *Phys. Rev. D* **100**, no.9, 094028 (2019)
- [29] H. X. Chen, W. Chen and S. L. Zhu, *Phys. Rev. D* **100**, no.5, 051501 (2019)
- [30] T. J. Burns and E. S. Swanson, *Phys. Rev. D* **100**, no.11, 114033 (2019)
- [31] M. L. Du, V. Baru, F. K. Guo, C. Hanhart, U. G. Meißner, J. A. Oller and Q. Wang, *Phys. Rev. Lett.* **124**, no.7, 072001 (2020)
- [32] B. Wang, L. Meng and S. L. Zhu, *JHEP* **11**, 108 (2019)
- [33] R. Chen, J. He and X. Liu, *Chin. Phys. C* **41**, no.10, 103105 (2017)
- [34] E. Santopinto and A. Giachino, *Phys. Rev. D* **96**, no.1, 014014 (2017)
- [35] C. W. Shen, J. J. Wu and B. S. Zou, *Phys. Rev. D* **100**, no.5, 056006 (2019)
- [36] C. W. Xiao, J. Nieves and E. Oset, *Phys. Lett. B* **799**, 135051 (2019)
- [37] B. Wang, L. Meng and S. L. Zhu, *Phys. Rev. D* **101**, no.3, 034018 (2020)
- [38] H. X. Chen, L. S. Geng, W. H. Liang, E. Oset, E. Wang and J. J. Xie, *Phys. Rev. C* **93**, no.6, 065203 (2016)
- [39] R. Aaij *et al.* [LHCb], *Sci. Bull.* **66**, 1278-1287 (2021)
- [40] R. Aaij *et al.* [LHCb], *Phys. Rev. Lett.* **128** (2022), 062001
- [41] R. Aaij *et al.* [LHCb], [arXiv:2109.01056 [hep-ex]].
- [42] R. Aaij *et al.* [LHCb], [arXiv:2109.01038 [hep-ex]].
- [43] J. Carlson, L. Heller and J. A. Tjon, *Phys. Rev. D* **37**, 744 (1988)
- [44] B. A. Gelman and S. Nussinov, *Phys. Lett. B* **551**, 296-304 (2003)
- [45] J. Vijande, F. Fernandez, A. Valcarce and B. Silvestre-Brac, *Eur. Phys. J. A* **19**, 383 (2004)
- [46] Y. Cui, X. L. Chen, W. Z. Deng and S. L. Zhu, *HEP NP* **31**, 7-13 (2007)
- [47] F. S. Navarra, M. Nielsen and S. H. Lee, *Phys. Lett. B* **649**, 166-172 (2007) doi:10.1016/j.physletb.2007.04.010
- [48] J. Vijande, E. Weissman, A. Valcarce and N. Barnea, *Phys. Rev. D* **76**, 094027 (2007)
- [49] D. Ebert, R. N. Faustov, V. O. Galkin and W. Lucha, *Phys. Rev. D* **76**, 114015 (2007)
- [50] S. H. Lee and S. Yasui, *Eur. Phys. J. C* **64**, 283-295 (2009)
- [51] Z. G. Wang, *Acta Phys. Polon. B* **49** (2018), 1781
- [52] Y. Yang, C. Deng, J. Ping and T. Goldman, *Phys. Rev. D* **80**, 114023 (2009)
- [53] M. L. Du, W. Chen, X. L. Chen and S. L. Zhu, *Phys. Rev. D* **87**, no.1, 014003 (2013)
- [54] S. Q. Luo, K. Chen, X. Liu, Y. R. Liu and S. L. Zhu, *Eur. Phys. J. C* **77**, no.10, 709 (2017)
- [55] M. Karliner and J. L. Rosner, *Phys. Rev. Lett.* **119**, no.20, 202001 (2017)
- [56] E. J. Eichten and C. Quigg, *Phys. Rev. Lett.* **119**, no.20, 202002 (2017)
- [57] S. Sakai, L. Roca and E. Oset, *Phys. Rev. D* **96**, no.5, 054023 (2017)
- [58] A. V. Manohar and M. B. Wise, *Nucl. Phys. B* **399** (1993), 17-33
- [59] S. Pepin, F. Stancu, M. Genovese and J. M. Richard, *Phys. Lett. B* **393** (1997), 119-123
- [60] D. Janc and M. Rosina, *Few Body Syst.* **35** (2004), 175-196
- [61] Y. Ikeda, B. Charron, S. Aoki, T. Doi, T. Hatsuda, T. Inoue, N. Ishii, K. Murano, H. Nemura and K. Sasaki, *Phys. Lett. B* **729**, 85-90 (2014)
- [62] T. F. Carames, A. Valcarce and J. Vijande, *Phys. Lett. B* **699**, 291-295 (2011)
- [63] R. Molina, T. Branz and E. Oset, *Phys. Rev. D* **82** (2010), 014010
- [64] N. Li, Z. F. Sun, X. Liu and S. L. Zhu, *Phys. Rev. D* **88** (2013) no.11, 114008
- [65] G. Q. Feng, X. H. Guo and B. S. Zou, [arXiv:1309.7813 [hep-ph]].
- [66] P. Junnarkar, N. Mathur and M. Padmanath, *Phys. Rev. D* **99** (2019) no.3, 034507
- [67] L. Maiiani, A. D. Polosa and V. Riquer, *Phys. Rev. D* **100** (2019) no.7, 074002
- [68] B. Wang, Z. W. Liu and X. Liu, *Phys. Rev. D* **99**, no.3, 036007 (2019).
- [69] M. Z. Liu, T. W. Wu, M. Pavon Valderrama, J. J. Xie and L. S. Geng, *Phys. Rev. D* **99** (2019) no.9, 094018
- [70] R. L. Jaffe, *Phys. Rev. Lett.* **38** (1977), 195-198.
- [71] A. P. Balachandran, A. Barducci, F. Lizzi, V. G. J. Rodgers and A. Stern, *Phys. Rev. Lett.* **52** (1984), 887
- [72] H. Takahashi, J. K. Ahn, H. Akikawa, S. Aoki, K. Arai, S. Y. Bahk, K. M. Baik, B. Bassalleck, J. H. Chung and M. S. Chung, *et al. Phys. Rev. Lett.* **87** (2001), 212502
- [73] H. Polinder, J. Haidenbauer and U. G. Meissner, *Phys. Lett. B* **653** (2007), 29-37
- [74] C. J. Yoon, H. Akikawa, K. Aoki, Y. Fukao, H. Funahashi, M. Hayata, K. Imai, K. Miwa, H. Okada and N. Saito, *et al. Phys. Rev. C* **75** (2007), 022201
- [75] T. Inoue *et al.* [HAL QCD], *Phys. Rev. Lett.* **106** (2011), 162002
- [76] S. R. Beane *et al.* [NPLQCD], *Phys. Rev. Lett.* **106** (2011), 162001
- [77] K. Morita, T. Furumoto and A. Ohnishi, *Phys. Rev. C* **91** (2015) no.2, 024916
- [78] K. W. Li, T. Hyodo and L. S. Geng, *Phys. Rev. C* **98** (2018) no.6, 065203
- [79] N. Lee, Z. G. Luo, X. L. Chen and S. L. Zhu, *Phys. Rev. D* **84** (2011), 014031
- [80] H. Garcilazo and A. Valcarce, *Eur. Phys. J. C* **80** (2020) no.8, 720
- [81] S. M. Gerasyuta and E. E. Matskevich, *Int. J. Mod. Phys. E* **21** (2012), 1250058
- [82] F. Froemel, B. Julia-Diaz and D. O. Riska, *Nucl. Phys. A* **750** (2005), 337-356
- [83] Z. Xia, S. Fan, X. Zhu, H. Huang and J. Ping, *Phys. Rev. C* **105** (2022) no.2, 025201

- [84] X. K. Dong, F. K. Guo and B. S. Zou, *Commun. Theor. Phys.* **73** (2021) no.12, 125201
- [85] X. Z. Ling, M. Z. Liu and L. S. Geng, *Eur. Phys. J. C* **81** (2021) no.12, 1090
- [86] N. Li and S. L. Zhu, *Phys. Rev. D* **86** (2012), 014020
- [87] T. F. Carames and A. Valcarce, *Phys. Rev. D* **92** (2015) no.3, 034015
- [88] H. Huang, J. Ping and F. Wang, *Phys. Rev. C* **89** (2014) no.3, 035201
- [89] W. Meguro, Y. R. Liu and M. Oka, *Phys. Lett. B* **704**, 547-550 (2011).
- [90] X. W. Wang, Z. G. Wang and G. I. Yu, *Eur. Phys. J. A* **57** (2021) no.9, 275
- [91] R. Chen, A. Hosaka and X. Liu, *Phys. Rev. D* **96** (2017) no.11, 116012
- [92] J. X. Lu, L. S. Geng and M. P. Valderrama, *Phys. Rev. D* **99** (2019) no.7, 074026
- [93] V. Bernard, N. Kaiser and U. G. Meissner, *Int. J. Mod. Phys. E* **4** (1995), 193-346
- [94] E. Epelbaum, H. W. Hammer and U. G. Meissner, *Rev. Mod. Phys.* **81** (2009), 1773-1825
- [95] R. Machleidt and D. R. Entem, *Phys. Rept.* **503** (2011), 1-75
- [96] U. G. Meißner, *Phys. Scripta* **91** (2016) no.3, 033005
- [97] H. W. Hammer, S. König and U. van Kolck, *Rev. Mod. Phys.* **92** (2020) no.2, 025004
- [98] B. L. Huang, Z. Y. Lin and S. L. Zhu, *Phys. Rev. D* **105** (2022) no.3, 036016
- [99] H. Xu, B. Wang, Z. W. Liu and X. Liu, *Phys. Rev. D* **99** (2019) no.1, 014027
- [100] K. Chen, R. Chen, L. Meng, B. Wang and S. L. Zhu, [[arXiv:2109.13057](https://arxiv.org/abs/2109.13057)] [[hep-ph](#)].
- [101] K. Chen, B. Wang and S. L. Zhu, [[arXiv:2112.13203](https://arxiv.org/abs/2112.13203)] [[hep-ph](#)].
- [102] L. Meng, B. Wang and S. L. Zhu, *Phys. Rev. C* **101**, no.6, 064002 (2020)
- [103] B. Wang, L. Meng and S. L. Zhu, *Phys. Rev. D* **101**, no.9, 094035 (2020)
- [104] S. Scherer, *Adv. Nucl. Phys.* **27** (2003), 277 [[arXiv:hep-ph/0210398](https://arxiv.org/abs/hep-ph/0210398)] [[hep-ph](#)].
- [105] H. Y. Cheng, C. Y. Cheung, G. L. Lin, Y. C. Lin, T. M. Yan and H. L. Yu, *Phys. Rev. D* **47**, 1030-1042 (1993).
- [106] Z. W. Liu and S. L. Zhu, *Phys. Rev. D* **86**, 034009 (2012).
- [107] Y. R. Liu and M. Oka, *Phys. Rev. D* **85**, 014015 (2012).
- [108] L. Meng, G. J. Wang, C. Z. Leng, Z. W. Liu and S. L. Zhu, *Phys. Rev. D* **98**, no.9, 094013 (2018).
- [109] Z. F. Sun, Z. G. Luo, J. He, X. Liu and S. L. Zhu, *Chin. Phys. C* **36** (2012), 194-204
- [110] C. Ordonez, L. Ray and U. van Kolck, *Phys. Rev. C* **53** (1996), 2086-2105
- [111] E. Epelbaum, W. Gloeckle and U. G. Meissner, *Nucl. Phys. A* **671** (2000), 295-331
- [112] B. Borasoy, *Eur. Phys. J. C* **8** (1999), 121-130
- [113] J. F. Donoghue and B. R. Holstein, [[arXiv:hep-ph/9803312](https://arxiv.org/abs/hep-ph/9803312)] [[hep-ph](#)].
- [114] J. F. Donoghue, B. R. Holstein and B. Borasoy, *Phys. Rev. D* **59** (1999), 036002